

---

# Self-Adaptive Physics-Informed Neural Networks using a Soft Attention Mechanism

---

**Levi D. McCleeny\***   **Ulisses Braga-Neto**  
 Department of Electrical and Computer Engineering  
 Texas A&M University  
 College Station, TX USA  
 {levimccleeny,ulisses}@tamu.edu

## Abstract

Physics-Informed Neural Networks (PINNs) have emerged recently as a promising application of deep neural networks to the numerical solution of nonlinear partial differential equations (PDEs). However, it has been observed that the original PINN algorithm can produce inaccuracies around sharp transitions in the solution, as well as display instability during training. This has prompted recent efforts in developing adaptive algorithms for PINNs. This paper introduces self-adaptive PINNs, a novel algorithm based on a simple soft attention mechanism that requires no extra hyperparameters. Self-adaptive PINNs are based on trainable weights that can automatically force the neural network to focus on difficult regions of the solution. We demonstrate the performance of the proposed self-adaptive PINN algorithm in the solution of the Allen-Cahn PDE, which displays sharp space and time transitions.

## 1 Introduction

Physics-Informed Neural Networks (PINNs) have recently emerged as a very promising application of deep neural networks in engineering and science [1], as part of the broader field of scientific machine learning [2]. PINNs are powerful function approximators [3, 4], made possible by recent advances in GPU capabilities and training algorithms for deep neural networks [5, 6], as well as the invention of automatic differentiation methods [7, 8], which can be used to solve ordinary [9], partial [10], or stochastic [11] differential equations.

A great advantage of PINNs over traditional time-step solvers is that the entire spatial-temporal domain can be solved at once using collocation points distributed irregularly (rather than on a grid) across the spatial-temporal domain, in a process that can be massively parallelized via GPU. As we have continued to see GPU capabilities increase in recent years, a method that relies on parallelism in training iterations will likely emerge as the predominant approach in scientific computing.

The original continuous PINN algorithm proposed in [1], henceforth referred to as the “baseline PINN” algorithm, is effective at estimating solutions that are reasonably smooth, such as Burger’s equation, the wave equation, Poisson’s equation, and Schrodinger’s equation. On the other hand, it has been observed that the baseline PINN has trouble in convergence and accuracy when the solution contains sharp and intricate space and time transitions [12, 13]. This is the case, for example, of the Allen-Cahn and Cahn-Hilliard equations of phase-field models [12].

To address this issue, various modifications of the baseline PINN algorithm have been proposed. For example, in [12], a series of schemes are introduced, including nonadaptive weighting of the training loss function, adaptive resampling of the collocation points, and partitioning of the time axis, while

---

\*levimccleeny@tamu.edu, levimccleeny.com

in [13], a learning rate annealing scheme was proposed. The consensus has been that adaptation mechanisms are essential to make PINNs more stable and able to approximate well difficult regions of the solution.

This paper introduces self-adaptive PINNs, a simple solution to the adaptation problem for solving partial difference equations (PDEs), which uses trainable weights as a soft multiplicative mask reminiscent of the attention mechanism used in computer vision [14, 15]. The weights are trained concurrently with the approximation network. As a result, initial, boundary or collocation points in difficult regions of the solution are automatically weighted more in the loss function, forcing the approximation to improve on those points. Preliminary experimental results show that self-adaptive PINNs can solve PDEs with complex solutions, such as the Allen Cahn PDE, accurately and fast.

## 2 Background

### 2.1 Overview of Physics-Informed Neural Networks

Typical black-box deep learning methodologies do not take into account physical understanding of the problem domain. The PINN approach is based on constraining the output of a deep neural network to satisfy a physical model in addition to sample data (if any).

Consider a general nonlinear PDE of the form:

$$u_t + \mathcal{N}_x[u] = 0, \quad \mathbf{x} \in \Omega, \quad t \in [0, T], \quad (1)$$

$$u(\mathbf{x}, 0) = h(\mathbf{x}), \quad \mathbf{x} \in \Omega, \quad (2)$$

$$u(\mathbf{x}, t) = g(\mathbf{x}, t), \quad \mathbf{x} \in \partial\Omega, \quad t \in [0, T], \quad (3)$$

where  $\mathbf{x} \in \Omega$  is a spatial vector variable in a domain  $\Omega \subset \mathbb{R}^d$ ,  $t$  is time, and  $\mathcal{N}_x$  is a spatial differential operator. Following [1], let  $u(\mathbf{x}, t)$  be approximated by the output  $u_\theta(\mathbf{x}, t)$  of a deep neural network with inputs  $\mathbf{x}$  and  $t$ . Define the residual as:

$$r_\theta(\mathbf{x}, t) := \frac{\partial}{\partial t} u_\theta(\mathbf{x}, t) + \mathcal{N}_x[u_\theta(\mathbf{x}, t)], \quad (4)$$

where all partial derivatives can be computed by automatic differentiation methods [7, 8]. The parameters  $\theta$  are trained by back-propagation [16] on a loss function that penalizes the output for not satisfying (1)-(3):

$$\mathcal{L}(\theta) = \mathcal{L}_r(\theta) + \mathcal{L}_b(\theta) + \mathcal{L}_0(\theta), \quad (5)$$

where  $\mathcal{L}_r$  is the residual loss from 4 and, for initial and boundary value problems,  $\mathcal{L}_{u_b}$  and  $\mathcal{L}_{u_0}$  are the boundary and initial condition losses, respectively. These individual loss functions take the form:

$$\mathcal{L}_r(\theta) = \frac{1}{N_r} \sum_{i=1}^{N_r} r(\mathbf{x}_r^i, t_r^i)^2, \quad (6)$$

$$\mathcal{L}_b(\theta) = \frac{1}{N_b} \sum_{i=1}^{N_b} |u(\mathbf{x}_b^i, t_b^i) - g_b^i|^2, \quad (7)$$

$$\mathcal{L}_0(\theta) = \frac{1}{N_0} \sum_{i=1}^{N_0} |u(\mathbf{x}_0^i, 0) - h_0^i|^2, \quad (8)$$

where  $\{\mathbf{x}_0^i, h_0^i = h(\mathbf{x}_0^i)\}_{i=1}^{N_0}$  are initial condition points,  $\{\mathbf{x}_b^i, t_b^i, g_b^i = g(\mathbf{x}_b^i, t_b^i)\}_{i=1}^{N_b}$  are boundary condition points,  $\{\mathbf{x}_r^i, t_r^i\}_{i=1}^{N_r}$  are collocation points randomly distributed in the domain  $\Omega$ , and  $N_0, N_b$  and  $N_r$  denote the total number of initial, boundary and collocation points, respectively. The parameters  $\theta$  can be tuned by minimizing the total training loss  $\mathcal{L}(\theta)$  via standard gradient descent procedures used in deep learning.

### 2.2 Related Work

The baseline PINN algorithm can be unstable during training and produce inaccurate approximations around sharp space and time transitions in the solution. Much of the recent literature on PINNs has been devoted to mitigating these issues by introducing modifications to the baseline PINN algorithm that can increase training stability and accuracy of the approximation. We mention some of these approaches below.

**Nonadaptive Weighting.** In [12], it was pointed out that a premium should be put on forcing the neural network to satisfy the initial conditions closely, especially for PDEs describing time-irreversible processes, where the solution has to be approximated well early. Accordingly, a loss function of the form  $\mathcal{L}(\theta) = \mathcal{L}_r(\theta) + \mathcal{L}_b(\theta) + C \mathcal{L}_0(\theta)$  was suggested, where  $C \gg 1$  is a hyperparameter.

**Learning Rate Annealing.** In [13], it is argued that the optimal value of the weight  $C$  in the previous scheme may vary wildly among different PDEs so that choosing its value would be difficult. Instead they propose to use weights that are tuned during training using statistics of the backpropagated gradients of the loss function. It is noteworthy that the weights themselves are not adjusted by backpropagation. Instead, they behave as learning rate coefficients, which are updated after each epoch of training.

**Adaptive Resampling.** In [12], a strategy to adaptively resample the residual collocation points based on the magnitude of the residual is proposed. While this approach improves the approximation, the training process must be interrupted and the MSE evaluated on the residual points to deterministically resample the ones with the highest error. After each resampling step, the number of residual points grows, increasing computational complexity.

**Stochastic Gradient Descent.** A training procedure where a different subset of collocation points are randomly sampled at each iteration was proposed by [13]. While stochastic gradient descent approaches a global minimum in an infinite limit [17], it is a random method that relies on sufficient random sampling and a large training horizon, which may be computationally intractable.

**Partitioning of the Time Axis.** In [12], another method is suggested, which simply divides the time axis into several smaller intervals, and trains PINNs separately on them, either sequentially or in parallel. This approach is time-consuming due to the need to train multiple PINNs.

**Neural Tangent Kernel (NTK) Weighting.** Most recently, [18] introduced weights on the collocation and boundary losses, which are updated via neural tangent kernels. This approach derives a deterministic kernel which remains constant during training.

### 3 Methods

While the methods outlined in the previous section produce improvements in stability and accuracy over the baseline PINN, they are either nonadaptive or require brute-force adaptation at increased computational cost. Here we propose a simple procedure that uses fully-trainable weights and require no extra hyperparameters. Unlike the previous approaches, the weights in the loss function are updated by backpropagation together with the network weights. In effect, the weights behave as a multiplicative soft attention mask, in a way that is reminiscent of attention mechanisms used in computer vision [14, 15].

Self-adaptive PINN utilizes the following loss function

$$\mathcal{L}(\theta, \mathbf{w}_r, \mathbf{w}_b, \mathbf{w}_0) = \mathcal{L}_r(\theta, \mathbf{w}_r) + \mathcal{L}_b(\theta, \mathbf{w}_b) + \mathcal{L}_0(\theta, \mathbf{w}_0), \quad (9)$$

where  $\mathbf{w}_r = (w_r^1, \dots, w_r^{N_r})$ ,  $\mathbf{w}_b = (w_b^1, \dots, w_b^{N_b})$ , and  $\mathbf{w}_0 = (w_0^1, \dots, w_0^{N_0})$  are vectors of weights for the initial, boundary, and collocation points, respectively, and

$$\mathcal{L}_r(\theta, \mathbf{w}_r) = \frac{1}{N_r} \sum_{i=1}^{N_r} [w_r^i r(\mathbf{x}_r^i, t_r^i)]^2 \quad (10)$$

$$\mathcal{L}_b(\theta, \mathbf{w}_b) = \frac{1}{N_b} \sum_{i=1}^{N_b} [w_b^i (u(\mathbf{x}_b^i, t_b^i) - g_b^i)]^2 \quad (11)$$

$$\mathcal{L}_0(\theta, \mathbf{w}_0) = \frac{1}{N_0} \sum_{i=1}^{N_0} [w_0^i (u(\mathbf{x}_0^i, 0) - h_0^i)]^2. \quad (12)$$

The trainable weights can efficiently force the network to focus on the initial, boundary, or residual points located in difficult or important regions of the solution. Any of the weights can be set to fixed,

non-trainable values, if desired. For example, by setting  $w_b^i \equiv 1$ , only the weights of the initial and residual points would be trained.

In our implementation, the self-adaptive PINN parameters  $(\theta, \mathbf{w}_r, \mathbf{w}_b, \mathbf{w}_0)$  are trained via a fixed number of iterations of adam [19] followed by another fixed number of iterations of L-BFGS quasi-newton method [20]. This is consistent with the baseline PINN formulation in [1], as well as follow-up literature [12]. However, the adaptive weights are only updated in the Adam training steps, and are held constant during L-BFGS training, in order to reduce the computational burden and speed up training.

## 4 Results

In this section we present experimental results that assess the accuracy of the approximation obtained with the self-adaptive PINN algorithm against an expensive high-fidelity numerical solution, using the Allen-Cahn PDE. We remark that we applied the baseline PINN and the nonadaptive weighted scheme in Section 2.2 with  $C = 100$  and observed that both failed in solving this PDE. (Our results, including shape of the approximation and L2-error, matched almost exactly those reported for these PINNs in [12].)

### 4.1 The Allen-Cahn Reaction-Diffusion System

The Allen-Cahn (AC) reaction-diffusion PDE is typically encountered in phase field models. The Allen-Cahn equation can be used, for instance, to simulate the phase separation process in the microstructure evolution of metallic alloys [21]. The AC initial value problem considered here is specified as follows:

$$u_t - 0.0001u_{xx} + 5u^3 - 5u = 0, \quad \mathbf{x} \in [-1, 1], \quad t \in [0, 1], \quad (13)$$

$$u(x, 0) = x^2 \cos(\pi x), \quad (14)$$

$$u(t, -1) = u(t, 1) \quad (15)$$

$$u_x(t, -1) = u_x(t, 1), \quad (16)$$

Research in phase-field systems described by PDEs such as Allen-Cahn is timely, due to its application in the emerging field of microstructure informatics in materials science and engineering [22].

The Allen-Cahn PDE is an interesting benchmark for PINNs for a variety of reasons. In challenges PINNs to approximate solutions with sharp space and time transitions with periodic boundary conditions (15, 16).

### 4.2 Experimental Setup

In order to deal with the periodic boundary conditions (15, 16), the boundary loss function  $\mathcal{L}_b(\theta, \mathbf{w}_b)$  in (11) is replaced by

$$\mathcal{L}_b(\theta, \mathbf{w}_b) = \frac{1}{N_b} \sum_{i=1}^{N_b} w_b^i (|u(1, t_b^i) - u(-1, t_b^i)|^2 + |u_x(1, t_b^i) - u_x(-1, t_b^i)|^2). \quad (17)$$

We compute the L2-error between the final approximation  $u(x, t)$  and a high-fidelity solution  $U(x, t)$  over a mesh  $\{x_i, t_i\}$  containing  $N_U = 201 \times 512$  points as

$$L_2 \text{ error} = \frac{\sqrt{\sum_{i=1}^{N_U} |u(x_i, t_i) - U(x_i, t_i)|^2}}{\sqrt{\sum_{i=1}^{N_U} |U(x_i, t_i)|^2}}. \quad (18)$$

The neural network architecture is fully connected with layer sizes  $[2, 100, 100, 100, 100, 1]$ . (The 2 inputs to the network are  $(x, t)$  pairs and the output is the approximated value of  $u_\theta$ .) We set the number of collocation, initial, and boundary points to  $N_r = 20,000$ ,  $N_0 = 100$  and  $N_b = 100$ , respectively (due to the periodic boundary condition, there are in fact 200 boundary points). Here we hold the boundary weights  $w_b^i$  at 1, while the initial weights  $w_0^i$  and collocation weights  $w_r^i$  are trained. The initial and collocation weights are initialized from a uniform distribution in the intervals  $[0, 100]$  and  $[0, 1]$ , respectively.

### 4.3 Plots and Discussion

Numerical results of the solution of the Allen-Cahn PDE by the self-adaptive PINN are displayed in figure 1. The top plot displays the approximation  $u(x, t)$  across the spatio-temporal domain and the initial and boundary collocation points. The middle plots show that the approximation is nearly identical to the high-fidelity solution  $U(x, t)$ . The average L2 error across 10 runs with random restarts was  $2.1\% \pm 1.21\%$ , beating the L2 errors reported in [12] with more complex adaptive methods that require more training iterations. The bottom left plot displays the residual  $r(u, t)$  across the spatio-temporal domain, showing that it is very close to zero. Finally, the bottom right plot displays the absolute difference between approximation and high-fidelity solution, where we can see that the approximation is excellent in most points of the domain, with the largest errors still in the locations of the solution with the sharpest transitions.

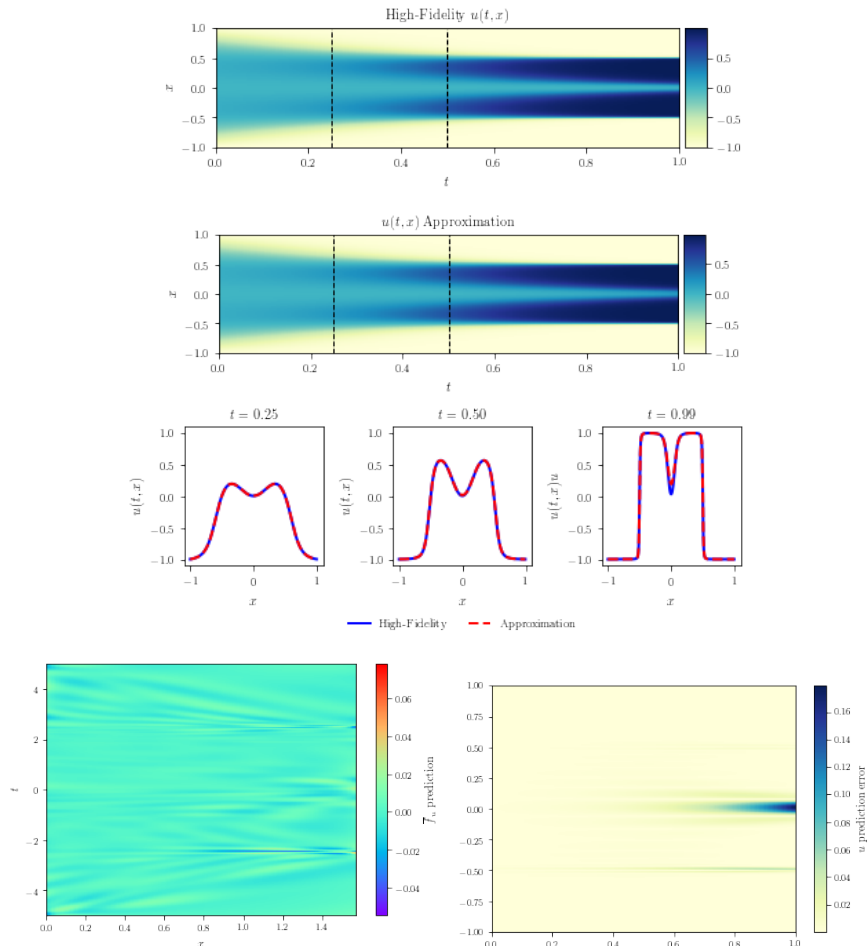


Figure 1: *Top:* Plots of the High-Fidelity and Approximation  $u(x, t)$  via the self-adaptive PINN. *Middle:* Snapshots of the approximation  $u(x, t)$  vs. the high-fidelity solution  $U(x, t)$  at various time points through the temporal evolution. *Bottom Left:* Residual  $r(x, t)$  across the spatial-temporal domain. *Bottom Right:* Absolute error between approximation and high-fidelity solution across the spatial-temporal domain.

Figure 2 is unique to the proposed self-adaptive PINN algorithm. It displays the trained weights for the collocation points across the spatio-temporal domain. These are the weights of the multiplicative soft attention mask self-imposed by the PINN. This plot stays remarkably constant across different runs with random restarts, which is an indication that it is a property of the particular PDE being solved. We can observe that in this case, more attention is needed early in the solution. In [12], this observation was justified by the fact that the Allen-Cahn PDEs describes a time-irreversible

diffusion-reaction processes, where the solution has to be approximated well early. However, here this fact is “discovered” by the self-adaptive PINN itself.

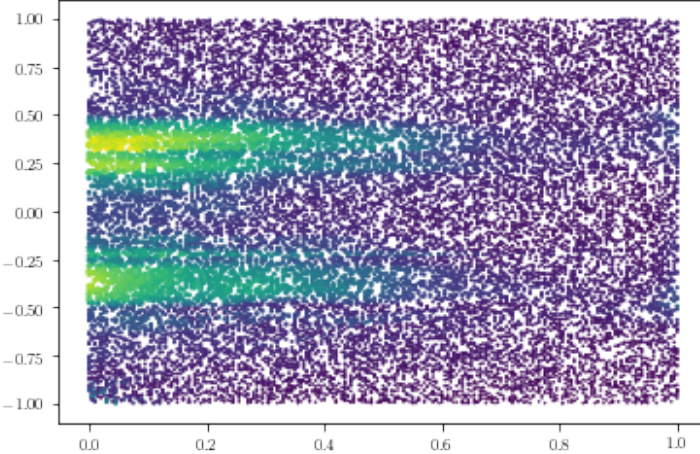


Figure 2: Learned weights across the spatio-temporal domain. Brighter colors and larger points indicate larger weights.

#### 4.4 Conclusion

In this paper, we introduced a novel self-adaptive PINN algorithm. This approach uses a similar conceptual framework as soft self-attention mechanisms used in Computer Vision, in that the network identifies which inputs are most important to its own training, in real time, with no additional hyperparameters. These weights are updated with respect to the loss function of the PINN, therefore the PINN training is capable of identifying a unique mask for any initial value problem.

Self-adaptive PINNs allow for more accurate solutions of PDEs with smaller computational cost than other adaptive PINN algorithms. It avoids the discretization step of classical PDE solvers and some PINN algorithms. The methodology was applied to an Allen-Cahn PDE, where it is shown that it achieves an approximation that is almost identical to a high-fidelity solution (at a reduced computational cost). We believe that self-adaptive PINNs open up new possibilities for the use of deep neural networks as fast solvers for complex nonlinear PDEs in engineering and science.

#### Acknowledgments

The authors would like to acknowledge the support of the D<sup>3</sup>EM program funded through NSF Award DGE-1545403. The authors would further like to thank the US Army CCDC Army Research Lab for their generous support and affiliation.

#### References

- [1] Maziar Raissi, Paris Perdikaris, and George E Karniadakis. Physics-informed neural networks: A deep learning framework for solving forward and inverse problems involving nonlinear partial differential equations. *Journal of Computational Physics*, 378:686–707, 2019.
- [2] Christopher Rackauckas, Yingbo Ma, Julius Martensen, Collin Warner, Kirill Zubov, Rohit Supekar, Dominic Skinner, and Ali Ramadhan. Universal differential equations for scientific machine learning. *arXiv preprint arXiv:2001.04385*, 2020.
- [3] Jooyoung Park and Irwin W Sandberg. Universal approximation using radial-basis-function networks. *Neural computation*, 3(2):246–257, 1991.
- [4] Kurt Hornik, Maxwell Stinchcombe, and Halbert White. Universal approximation of an unknown mapping and its derivatives using multilayer feedforward networks. *Neural networks*, 3(5):551–560, 1990.

- [5] Martín Abadi, Paul Barham, Jianmin Chen, Zhifeng Chen, Andy Davis, Jeffrey Dean, Matthieu Devin, Sanjay Ghemawat, Geoffrey Irving, Michael Isard, et al. Tensorflow: A system for large-scale machine learning. In *12th {USENIX} symposium on operating systems design and implementation ({OSDI} 16)*, pages 265–283, 2016.
- [6] Jarrett Revels, Miles Lubin, and Theodore Papamarkou. Forward-mode automatic differentiation in julia. *arXiv preprint arXiv:1607.07892*, 2016.
- [7] Atılım Güneş Baydin, Barak A Pearlmutter, Alexey Andreyevich Radul, and Jeffrey Mark Siskind. Automatic differentiation in machine learning: a survey. *The Journal of Machine Learning Research*, 18(1):5595–5637, 2017.
- [8] Adam Paszke, Sam Gross, Soumith Chintala, Gregory Chanan, Edward Yang, Zachary DeVito, Zeming Lin, Alban Desmaison, Luca Antiga, and Adam Lerer. Automatic differentiation in pytorch. 2017.
- [9] Ricky TQ Chen, Yulia Rubanova, Jesse Bettencourt, and David K Duvenaud. Neural ordinary differential equations. In *Advances in neural information processing systems*, pages 6571–6583, 2018.
- [10] Jiequn Han, Arnulf Jentzen, and E Weinan. Solving high-dimensional partial differential equations using deep learning. *Proceedings of the National Academy of Sciences*, 115(34):8505–8510, 2018.
- [11] Maziar Raissi. Forward-backward stochastic neural networks: Deep learning of high-dimensional partial differential equations. *arXiv preprint arXiv:1804.07010*, 2018.
- [12] Colby L Wight and Jia Zhao. Solving allen-cahn and cahn-hilliard equations using the adaptive physics informed neural networks. *arXiv preprint arXiv:2007.04542*, 2020.
- [13] Sifan Wang, Yujun Teng, and Paris Perdikaris. Understanding and mitigating gradient pathologies in physics-informed neural networks. *arXiv preprint arXiv:2001.04536*, 2020.
- [14] Fei Wang, Mengqing Jiang, Chen Qian, Shuo Yang, Cheng Li, Honggang Zhang, Xiaogang Wang, and Xiaou Tang. Residual attention network for image classification. In *Proceedings of the IEEE conference on computer vision and pattern recognition*, pages 3156–3164, 2017.
- [15] Yanwei Pang, Jin Xie, Muhammad Haris Khan, Rao Muhammad Anwer, Fahad Shahbaz Khan, and Ling Shao. Mask-guided attention network for occluded pedestrian detection. In *Proceedings of the IEEE International Conference on Computer Vision*, pages 4967–4975, 2019.
- [16] Yves Chauvin and David E Rumelhart. *Backpropagation: theory, architectures, and applications*. Psychology press, 1995.
- [17] Yi Zhou, Junjie Yang, Huihuai Zhang, Yingbin Liang, and Vahid Tarokh. Sgd converges to global minimum in deep learning via star-convex path. *arXiv preprint arXiv:1901.00451*, 2019.
- [18] Sifan Wang, Xinling Yu, and Paris Perdikaris. When and why pinns fail to train: A neural tangent kernel perspective. *arXiv preprint arXiv:2007.14527*, 2020.
- [19] Diederik P Kingma and Jimmy Ba. Adam: A method for stochastic optimization. *arXiv preprint arXiv:1412.6980*, 2014.
- [20] Dong C Liu and Jorge Nocedal. On the limited memory bfgs method for large scale optimization. *Mathematical programming*, 45(1-3):503–528, 1989.
- [21] Jie Shen and Xiaofeng Yang. Numerical approximations of allen-cahn and cahn-hilliard equations. *Discrete & Continuous Dynamical Systems-A*, 28(4):1669, 2010.
- [22] Courtney Kunselman, Vahid Attari, Levi McClenny, Ulisses Braga-Neto, and Raymundo Arroyave. Semi-supervised learning approaches to class assignment in ambiguous microstructures. *Acta Materialia*, 188:49–62, 2020.